

Growth of ultra thin vanadium dioxide thin films using magnetron sputtering

Fangfang Song¹ and B. E. White Jr.^{1, a)}

Department of Physics, Applied Physics, Astronomy, Binghamton University - State University of New York, Binghamton, NY, 13902

In this work, the results of fabricating ultra thin VO₂ films on the technologically relevant amorphous SiO₂ surface using reactive DC magnetron sputtering are presented. Results indicate that a post deposition anneal in low partial pressures of oxygen is an effective way at stabilizing the VO₂(M₁) phase on the SiO₂ surface. VO₂ films with a thickness of 42nm show a continuous microstructure, and undergo a resistivity change of more than a factor of 200 as the temperature of the film increases above 72°C. The film shows hysteresis in the metal-insulator transition temperature upon heating and cooling with a width of approximately 8°C. The resistivity of the low temperature semiconducting phase is found to be thermally activated with an activation energy 0.16±0.03 eV. Stress measurements using X-ray diffraction indicate that the ultra thin VO₂ film has a large tensile stress of 2.0±0.2 GPa. This value agrees well with the calculated thermal stress due to differential thermal expansion between the VO₂ thin film and silicon substrate. The stress leads to a shift of the metal-insulator transition temperature by approximately 4°C.

I. INTRODUCTION

Vanadium dioxide is a well known strongly correlated material whose electronic properties have been actively investigated experimentally^{1–6} and theoretically^{7–12}. The interest in VO₂ results from the abrupt change in resistivity (over several orders of magnitude in bulk crystals) that occurs at a transition temperature near room temperature (68°C). These features suggest numerous technological applications of VO₂, including novel memory devices^{13,14}, electronic switches^{15,16}, optical switches¹⁷, and sensors¹⁸.

However, the existence of a large number of distinct stable vanadium oxide phases offers a particular challenge to the growth of pure phase VO₂ thin films^{19,20}. Extensive effort has been undertaken for the high quality thin film processing of this material. VO₂ thin films have been successfully prepared by various techniques, including sputtering^{21–23}, chemical vapor deposition^{24–26}, pulsed

laser deposition^{27–29} and sol-gel coating^{30–32}. While the majority of the work in the literature has focused on growing thick VO₂ films (thickness > 100nm) under epitaxial growth conditions, relatively little has been reported on growing ultra thin vanadium oxide on an amorphous substrate. In addition, the literature indicates that growing high quality crystalline VO₂ films with thicknesses below 100nm is challenging. X. Wei argued that the crystallization of VO₂ deteriorates with decreasing film thickness and VO₂ films thinner than 100nm showed no obvious polycrystalline structure³³. D. Brassard et al. also report the discontinuous nature of VO₂ thin films when the film thickness is below 50nm³⁴. And Y. Park reported that a change of film thickness leads to a change of the crystalline phase and orientation of the vanadium oxide films³⁵.

Because the switching speed of many of the proposed VO₂ devices is proportional to the volume of VO₂ present, the ability to grow ultra thin films of the material while maintaining the metal-insulator transition is important. Incorporation of these new devices into exist-

^{a)}Electronic mail:bwhite@binghamton.edu

ing silicon based technology is made easier if these films can be produced on amorphous SiO_2 (a- SiO_2). In this paper, the investigation of the preparation of ultra thin VO_2 thin films on the technologically relevant SiO_2 surface by DC magnetron sputtering is presented. The results show that under proper deposition and post-annealing conditions, a factor of 200 change in resistivity can be achieved in films as thin as 42nm when deposited on an SiO_2 surface.

II. EXPERIMENTAL

The vanadium oxide thin films were deposited using a sputtering system made by AJA International. Thin films were sputtered from a 99.9% pure vanadium metal target on a silicon substrate on which a 100Å thermal SiO_2 had been grown. The deposition chamber was evacuated to a pressure of 1.33×10^{-4} Pa prior to heating the substrate. The deposition temperature was varied between 450°C to 550°C and the substrate was maintained at the desired temperature for 20 minutes for temperature stabilization. Pre-sputtering was performed for 10 minutes to clean the target. Reactively sputtered thin films were then deposited for a fixed deposition time of 10 minutes. During deposition, the pressure of the chamber was kept at 0.60 Pa. The Ar flow rate was set to be 20 sccm , and the O_2 flow rate was varied between 1.9 sccm and 3 sccm to vary the oxygen partial pressure. The DC power was maintained at 200 W , corresponding to a power density of 10.2 W/cm^2 across the 5 cm diameter target. After deposition, the samples were annealed in an oxygen atmosphere. The oxygen pressure was varied from 0 Pa to 4.80×10^{-2} Pa at an annealing temperature of 550°C .

The crystallographic phase of the thin films was determined by Glancing Incident X-ray Diffraction(GIXRD). During GIXRD, the angle of incidence was fixed at 0.6° ,

and the measurement was taken using a 2θ scan geometry. The thickness of the sample was determined using X-ray Reflectivity. X-ray diffraction was also used to measure the residual stress in the ultra thin VO_2 films. All diffraction scans were carried out using a PANalytical X'pert Pro Diffractometer with $\text{Cu } K_\alpha$ radiation. The microstructure of the thin films was investigated using a Zeiss Supra 55VP Field Emission Scanning Electron Microscope and a Veeco Multi-Techniques System 3100 Atomic Force Microscope with Nanoscope Voltage Controller. The electrical properties of the thin films were measured using a Keithley 4200 Semiconductor Characterization System.

III. RESULTS AND DISCUSSION

A. Effect of Deposition Conditions

1. Effect of Oxygen Partial Pressure

The impact of oxygen partial pressure on the phase of the reactively sputtered thin films was determined by varying the percentage of O_2 in the sputtering gas from 9% to 11% while maintaining the total pressure in the sputtering chamber at 0.60 Pa. This small change in O_2 concentration produced profound changes in the phase of the thin films. Figure 1 shows the GIXRD results of VO_x thin films deposited at slightly different oxygen partial pressure, while the substrate (thermally oxidized silicon) and deposition temperature (550°C) were held constant. When the percentage of oxygen in the sputtering ambient was 9%, two vanadium oxide phases were present in the films, V_3O_5 and V_2O_3 ; as the relative concentration of O_2 increased to 10%, the film was composed of V_7O_{13} , VO_2 and V_2O_5 ; a further increase in the relative oxygen concentration to 11% generates additional phases, including V_2O_5 , V_3O_7 , V_6O_{13} , V_2O_3 , and VO_2 . It

can be seen that high oxygen partial pressure does not necessarily lead to a more oxygen rich phase.

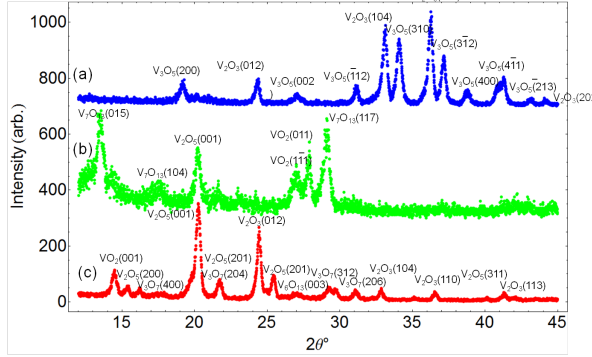


FIG. 1: GIXRD patterns of films prepared on same substrate (Si/SiO_2), same deposition temperature(550°C), but at different oxygen partial pressure,(a) 9% (b) 10% (c) 11%

2. Effect of Deposition Temperature

To investigate the impact of substrate temperature on the crystallographic morphology of the deposited films, the substrate temperature was varied from 450°C to 550°C while maintaining the O_2 partial pressure at 6.00×10^{-2} Pa. Figure 2 shows the GIXRD scans for the films prepared at different temperature. As shown in the figure, when the deposition temperature is 550°C , the film has two phases, V_2O_3 and V_3O_5 ; when the deposition temperature is 460°C , the film composition becomes $\text{V}_4\text{O}_9, \text{V}_3\text{O}_7, \text{V}_6\text{O}_{13}$ and V_2O_5 ; and when the deposition temperature is 450°C , the film has only one V_2O_3 phase. It can be seen that high substrate temperature does not necessarily produce an oxygen poor phase.

3. Effect of Substrate

To examine the impact of the substrate on the phases present in the thin films, two different substrates were

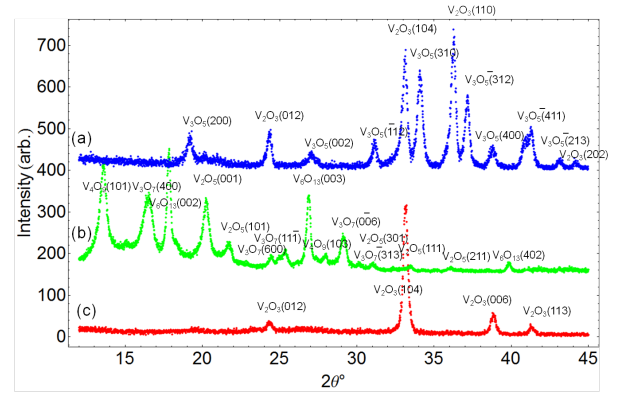


FIG. 2: GIXRD patterns of films prepared at same oxygen partial pressure(10%), on same substrate(Si/SiO_2), but at different temperature,(a) 550°C (b) 460°C (c) 450°C

explored, silicon and thermally oxidized silicon. Figure 3 shows the GIXRD pattern of samples prepared with the same deposition conditions but on different substrates (Si and oxidized silicon respectively). The deposition temperature was 450°C and the oxygen partial pressure was 6.00×10^{-2} Pa. It can be seen that the film is V_2O_3 on the oxidized silicon substrate, while $\text{VO}_2(\text{B})$ is formed on the Si substrate.

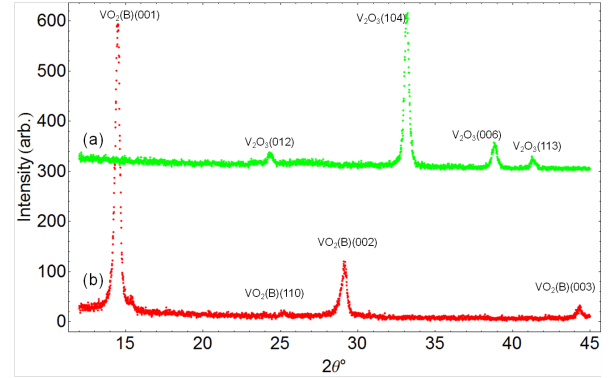


FIG. 3: GIXRD patterns of films prepared at same oxygen partial pressure(6.00×10^{-2} Pa), same temperature(450°C), but different substrate, (a) Si/SiO_2 (b) Si

B. Effect of Post Annealing Conditions

As shown in Figure 2, DC reactive sputtering under the explored conditions did not produce a pure VO_2 film on an amorphous SiO_2 surface. However, thin films of pure V_2O_3 were obtained on a-SiO₂ when the deposition temperature was 450°C with an oxygen partial pressure of 6.00×10^{-2} Pa. Thus efforts were taken to convert the V_2O_3 phase into VO_2 by post-deposition annealing the sample in an oxygen atmosphere. The oxygen pressure was varied from 0 Pa to 4.80×10^{-2} Pa at an annealing temperature of 550°C

Figure 4 shows the GIXRD data for the vanadium oxide films after being annealed at 550°C for 50 minutes under different oxygen pressures. After the film is annealed at 2.00×10^{-3} Pa of oxygen, all of the V_2O_3 peaks except for that of the (104) planes are observed to disappear. New peaks which are ascribed to the V_3O_5 phase appear. The peak at 30.20° corresponds to the V_4O_7 (122) plane. When the oxygen pressure becomes 6.70×10^{-3} Pa, no V_2O_3 peaks are observed. Only the V_4O_7 (122) peak and peaks ascribed to V_3O_5 are present. When the oxygen pressure increases to 1.33×10^{-2} Pa, peaks ascribed to the $\text{VO}_2(\text{M}1)$ phase appear. As the oxygen pressure is increased to 4.80×10^{-2} Pa, all the peaks are ascribed to VO_2 indicating that a single phase thin film of VO_2 has been obtained.

Below, Figure 5 shows the GIXRD pattern of VO_2 films after being annealed at 550°C at an with oxygen partial pressure of 4.80×10^{-2} Pa as a function of annealing time. After being annealed for 20 minutes, V_2O_3 peaks in the as deposited film are replaced by new peaks corresponding to the $\text{VO}_2(\text{M}1)$ phase. As the annealing time increases, no new phases appear, and the intensity of peaks associated with the $\text{VO}_2(\text{M}1)$ phase increases accompanied by decreases in the full width at half maximum (FWHM) of the peaks. This indicates grain growth

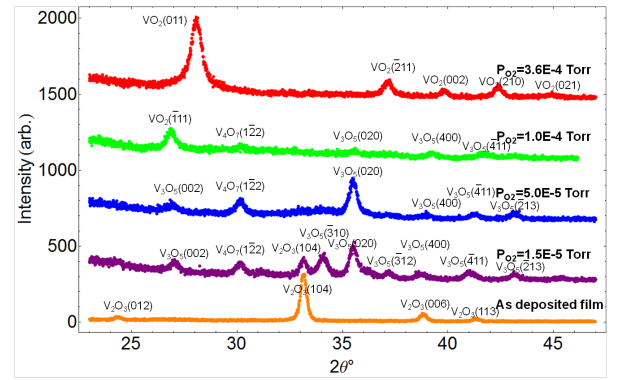


FIG. 4: GIXRD pattern of films after being annealed at different oxygen pressure

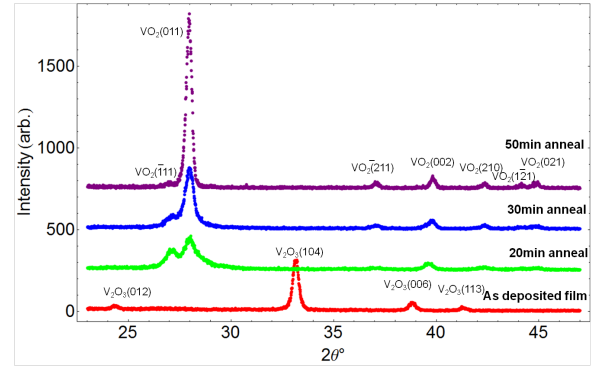


FIG. 5: GIXRD pattern of films after being annealed for different time

and an improvement of film crystallinity.

X-ray reflectivity was performed on the film after being annealed at 4.80×10^{-2} Pa O₂ atmosphere for 50 minutes to determine the film thickness. As shown in Figure 6, the green line is the experimental data and the red line is the fitted data. The fitting parameters are summarized in table I. Based on these data, the thickness is determined to be 42nm.

1. Microstructure of The Thin Films

Figure 7 below shows SEM images of the film after different annealing times. In the as deposited film, the

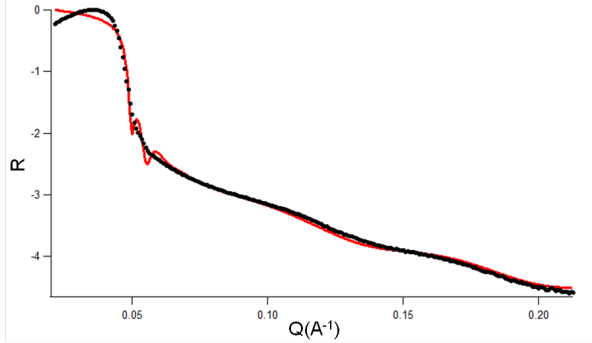


FIG. 6: X-ray reflectivity of the VO_2 film after being annealed at 4.80×10^{-2} Pa atmosphere for 50 minutes

TABLE I: Refelectedivity fitting parameter for VO_2 film

Layer	Material	Thickness(Å)	Roughness(Å)	Re[SLD] (\AA^{-2})
Layer 1	VO_2	422	55	4.5×10^{-5}
Substrate	SiO_2	-	0.2	2.6×10^{-5}

grains are uniform and densely packed with an average grain size of approximately 26.5nm . As the annealing time increases, grain growth is observed. Table II summarizes the average grain size as a function of annealing time.

TABLE II: Average grain size of vanadium oxide film after being annealed for different amount time

Annealing time(min)	As deposited	30	50
Average Grain Size(nm)	26.5	65.8	85.5

Figure 8 shows the AFM images of vanadium oxide films after being annealed for different amounts of time. And table III summarizes the Root Mean Square(RMS) roughness of these films. It can be seen that, going from as-deposited to being annealed for 30 minutes, the roughness of the film increases from 18.7\AA to 54.4\AA . After being annealed for 50 minutes, the roughness decreases to 43.5\AA .

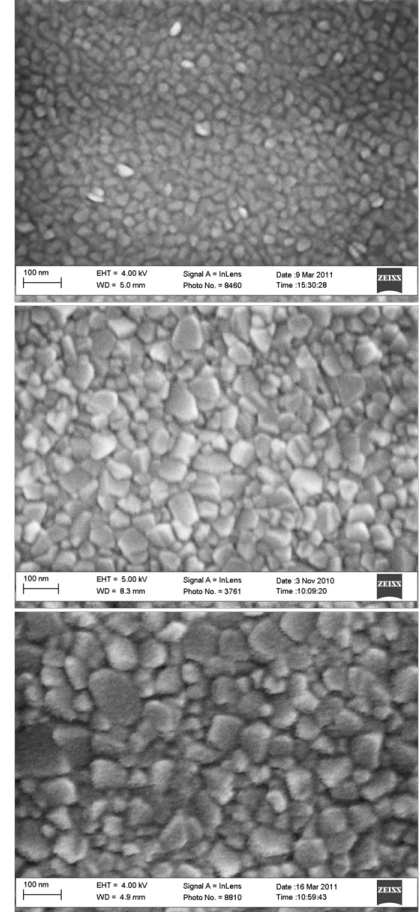


FIG. 7: SEM images of film after being annealed for different amount time (a) as deposited (b) 30 minutes (c) 50 minutes

TABLE III: RMS Roughness of vanadium oxide film after being annealed for different amount time

Annealing time(min)	As deposited	30	50
RMS Roughness(Å)	18.7	54.4	43.5

2. Temperature Dependence of Resistivity of The Thin Film

The nature of the hysteresis in the resistivity transition temperature of the VO_2 thin films after being annealed in 4.80×10^{-2} Pa O_2 atmosphere at 550°C for 50 min-

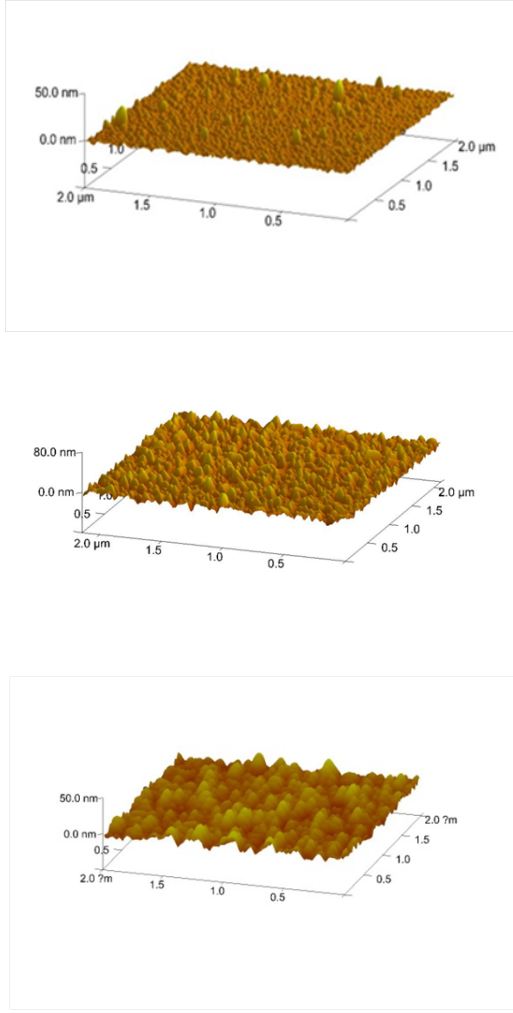


FIG. 8: AFM images of film after being annealed for different amount time (a) as deposited (b) 30 minutes (c) 50 minutes

utes was examined using a Keithley 4200 Semiconductor Characterization System with a four probe collinear configuration. Sample temperature was controlled using a JANIS Research ST-500 Cryogenic Probe Station. The sample temperature was increased from room temperature to 127°C followed by subsequent cooling back to room temperature.

The measured resistivity as a function of temperature is shown in figure 9. As can be seen in the figure, the transition temperature moves to higher temperatures when

the transition temperature is approached from the high temperature side of the data. The width of the hysteresis is estimated to be approximately 8°C , which is similar to the hysteresis width in VO_2 films epitaxially grown on sapphire approximately 6°C - 10°C .

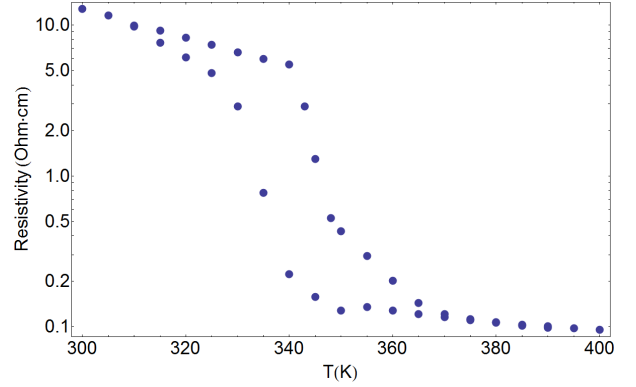
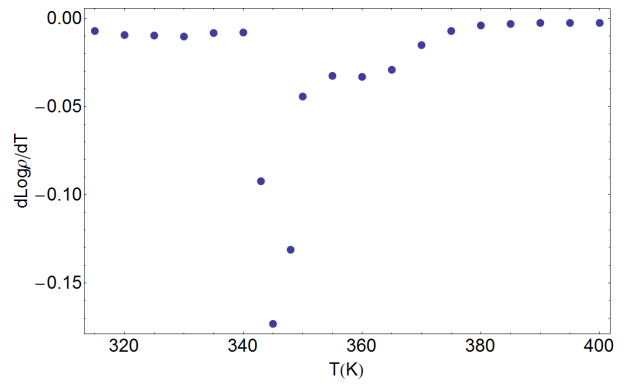


FIG. 9: Measured resistivity hysteresis curve of $\text{VO}_2(\text{M}_1)$ thin film

In order to precisely determine the transition temperature, we plot the $d(\log \rho)/dT$ vs. T for the heating cycle and the temperature at the minimum point of the curve is chosen to be the transition temperature³⁶. As shown in figure 10, the transition temperature is determined to be 72°C , which is higher than the reported value of 68°C on a sapphire substrate.



As shown in figure 9, the resistivity of the low tem-

perature monoclinic VO_2 phase on a a- SiO_2 substrate decreases as the temperature increases, which is a characteristic of a semiconductor. The temperature dependence of the resistivity has been observed to be thermally activated.

The activation energy for the conductivity is calculated using the Arrhenius equation:

$$\sigma = \sigma_a \exp(-E_a/kT) \quad (1)$$

Where E_a is the activation energy, σ is the conductivity of the film which is calculated using $\sigma = 1/\rho$, and σ_a is the pre-exponent factor.

Figure 11 shows the plot of $\ln \sigma$ as a function of $1/T$ in the temperature range from 27°C to 68°C . From the slope of the fitted line, the activation energy was calculated to be $0.16 \pm 0.03\text{ eV}$, in agreement with the reported value of 0.188 eV for VO_2 films grown on a Si substrate³⁷ and 0.12 eV for VO_2 films grown on a sapphire substrate³⁸. Although the temperature range is limited, Ref.³⁷ used a similar temperature range to calculate the activation energy.

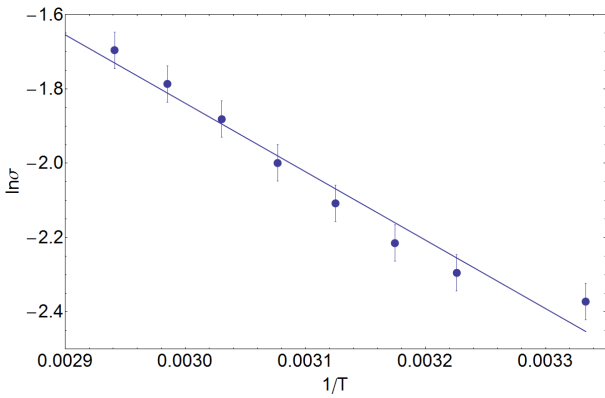


FIG. 11: $\ln \sigma$ vs. $1/T$ curve. The points are the measured data, and the solid line is the linear fitting line

C. Measurement of Residual Stress in the Films

Stress is believed to play an important role in the temperature of the resistivity transition of VO_2 ³⁹⁻⁴¹. Stress in the thin films of VO_2 was determined using the well-known $\sin^2(\psi)$ method⁴². This method takes advantage of the fact that when a stress is applied to a polycrystalline material, the material will be deformed elastically, and the lattice plane spacing in the constituent grains will change from their stress free value to some new value corresponding to the applied stress. The change of plane spacing causes a shift in the angles at which the diffraction peaks are observed in XRD to new 2θ positions. By measuring the 2θ position at different sample tilt angles ψ , which is the angle between the diffraction plane normal and the thin film surface normal, the residual stress can be calculated as⁴²:

$$\sigma_\phi = \frac{E}{(1+\nu)\sin^2\psi} \left(\frac{d_i - d_n}{d_n} \right) \quad (2)$$

Where d_n is the plane spacing at normal incidence under stress, d_i is the plane spacing when the incident beam is inclined at angle ψ to the surface normal, E is the Young's modulus, and ν is the Possion ratio.

The slope of a linear plot between $\frac{d_i - d_n}{d_n}$ and $\sin^2\psi$ equals $\frac{(1+\nu)\sigma_\phi}{E}$.

Although high 2θ peaks are usually preferred for higher strain sensitivity, the higher 2θ peaks are too weak and have shapes that are irregular, as shown in figure 5 for VO_2 films after being annealed at $4.80 \times 10^{-2}\text{ Pa O}_2$ for 50 minutes. Thus, the peak at $2\theta = 27.9^\circ$, which corresponds to diffraction from VO_2 (011) planes, was chosen for the stress measurement.

Figure 12 shows the XRD scan results with the incident beam inclined at different angles, ψ , to the surface normal. The grazing incident angle was set at 0.6° and those measurements were taken in the 2θ ranges from 26.5° to 29.5° using a 2θ scan geometry. It can be seen

that the 2θ peak shifts to a lower value as ψ increases. Table IV below summarize the 2θ position and calculated lattice spacing at different ψ .

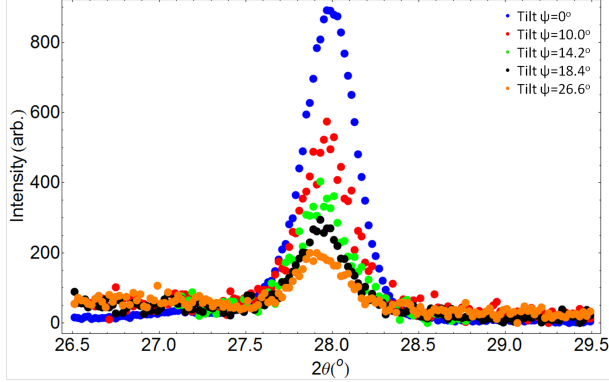


FIG. 12: GIXRD scan in range 26.5° - 29.5° with different tilt angle ψ

TABLE IV: Summarized measured 2θ position and calculated lattice spacing at different tilt angle ψ

$\sin^2\psi$	0	0.03	0.06	0.1	0.2
ψ	0	10.0	14.2	18.4	26.6
2θ	27.99	27.97	27.95	27.94	27.89
Lattice Spacing(d)	3.1851	3.1871	3.1902	3.1902	3.1965

Figure 13 is the plot of $\frac{d_i-d_n}{d_n}$ as a function of $\sin^2\psi$. The solid line is the best linear fit to the data. The slope of this line is found to be 0.018 ± 0.002 . Taking the VO_2 Young's modulus to be 140 GPa ⁴³, and Possion ratios to be 0.3, the stress in the VO_2 thin film is calculated to be $2.0 \pm 0.2 \text{ GPa}$. The positive slope of the $\frac{d_i-d_n}{d_n}$ vs. $\sin^2\psi$ plot indicates the stress is tensile.

As the thermal expansion coefficient of VO_2 is reported to be $2.1 \times 10^{-5}/\text{C}$ ⁴⁴, which is almost 10 times larger than that of Si, the film will contract more than the substrate when the film is cooled from 550°C to room temperature after annealing, producing a tensile stress in the film. Since the substrate is very thick compared to the film,

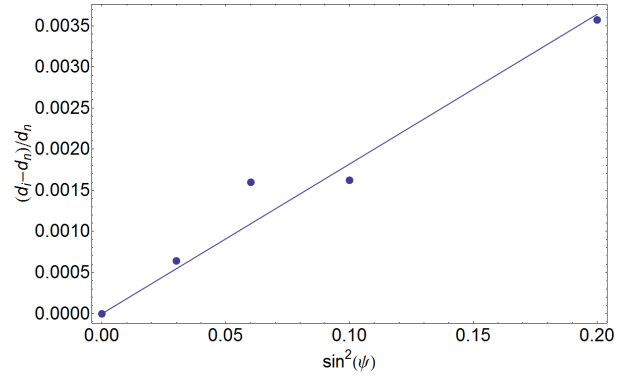


FIG. 13: Plot of $\frac{d_i-d_n}{d_n}$ as a function of $\sin^2\psi$, the solid line is the best linear fitting line

the equation for an infinitely thick substrate⁴⁵ can be used to calculate the thermal stress in the film:

$$\sigma_T = \int_{T_0}^{T_f} \Delta\alpha \frac{E}{1-\nu} dT = \Delta\bar{\alpha} \frac{E}{1-\nu} \Delta T = \frac{E}{1-\nu} \Delta\bar{\alpha} \Delta T \quad (3)$$

If we assume the thermal expansion coefficient of the VO_2 film and substrate do not vary with temperature, the calculated stress due to differential thermal expansion is found to be:

$$\begin{aligned} \sigma_T &= \frac{140 \text{ GPa}}{1-0.3} \times (2.1 \times 10^{-5} - 2.7 \times 10^{-6}) \times (550 - 25) \\ &= 1.92 \text{ GPa} \end{aligned} \quad (4)$$

This value agrees well the measured result, indicating that the residual stress in the VO_2 film mainly comes from thermal stress. In 2010, a stress-temperature phase diagram for the metal-insulator transition in VO_2 using a free-standing VO_2 nanobeam³⁹ was generated. This work indicates that the metal-insulator transition temperature should shift to higher values when the film is under tensile stress, as observed here.

IV. CONCLUSION

Preparation of ultra thin VO₂ films on the technologically relevant amorphous SiO₂ surface has been studied. The effect of oxygen partial pressure, deposition temperature and substrate on the film composition and crystal structure have been discussed. Post annealing in at low pressures of O₂ was found to stabilize the VO₂(M₁) phase.

VO₂ films with a thickness of 42nm show a continuous microstructure and undergo a resistivity change of more than a factor of 200 as the temperature increases above the metal-insulator transition temperature. The transition temperature was determined to be 72°C. The film shows hysteresis in the transition temperature when heating and cooling with a width of approximately 8°C. The activation energy of the low temperature semiconducting phase of the VO₂ film is determined to be 0.16 ± 0.03 eV. X-ray diffraction was used to measure the residual stress in the VO₂ films. Results indicate that the ultra thin VO₂ film has a large tensile stress of 2.0 ± 0.2 GPa. This value agrees well with that calculated thermal stress assuming differential thermal expansion between the VO₂ film and substrate. The stress is expected to lead to a shift of the metal-insulator transition temperature, as observed in the temperature dependent resistivity measurement.

V. ACKNOWLEDGEMENTS

We gratefully acknowledge the Center for Advanced Microelectronics Manufacturing at Binghamton University for support of this project. We are also indebted to Shijun Yu for assistance with the stress measurements in this work.

¹H. T. Kim, Y. W. Lee, B. J. Kim, B. J. Chae, S. J. Yun, K. Y. Kang, K. J. Han, K. J. Yae, and Y. S. Lim. Monoclinic and

correlated metal phase in VO₂ as evidence of the mott transition:coherent phonon analysis. *Phy. Rev. Lett.*, 97(26), 2006.

²A. Cavalleri, Th. Dekorsy, H. H. W Chong, J. C. Kieffer, and R. W. Schoenlein. Evidence for a structurally driven insulator to metal transition in VO₂: A view from the ultrafast timescale. *Phy. Rev. B*, 70(16), 2004.

³M. M. Qazilbash, M. Brehm, B. Chae, P. C. Ho, G. O. Andreev, B. Kim, S. J. Yun, A. V. Balatsky, and F. Keilmann. Mott transition in VO₂ revealed by infrared spectroscopy and nano-imaging. *Science*, 318(5857):1750–1753, 2007.

⁴C. N. Berglund and H. J. Gunnenheim. Electronic properties of VO₂ near the semiconductor-metal transition. *Phy. Rev.*, 185(3), 1969.

⁵A. S. Barker, H. W. Verleur, and H. J. Gunnenheim. Infrared optical properties of vanadium dioxide above and below the transition temperature. *Phy. Rev. Lett.*, 17(1286), 1966.

⁶E. E. Chain. The influence of deposition temperature on the structure and optical properties of vanadium-oxide films. *J. Vac. Sci. Technol.*, 4:432–435, 1986.

⁷D. Paquet and P. Hugon. Electron correlations and electron-lattice interactions in the metal-insulator, ferroelastic transition in VO₂: a thermodynamical study. *Phy. Rev. B*, 22(11):5284–5301, 1980.

⁸R. Wentzcovitch, W. Schulz, and P. Allen. VO₂ : Peierls or mott-hubbard? a view from band thoery. *Phy. Rev. Lett.*, 72(21):3389–3392, 1994.

⁹A. Zylbersztein and N. F. Mott. Metal-insulator tansition in vadium dioxide. *Phy. Rev. B*, 11(11):4393, 1975.

¹⁰M. Laad, L. Craco, and E. Muller-Hartmann. Metal-insulator tansition in rutile based VO₂. *Physica B*, 73, 2006.

¹¹H. T. Kim, B. J. Kim, Y. W. Lee, B. J. Chae, S. J. Yun, and K. Y. Kang. Hole driven MIT thoery, mott transition in VO₂,MoBRiK device. *Physica B*, 460:1076–1078, 2007.

¹²H. T. Kim, NewAuthor2, D. H. Youn, and S. L. Maeng. Mechanism and observation of mott transition in VO₂ based two and three terminal devices. *New Jour. of Phys.*, 6:52, 2004.

¹³T. Driscoll, H. T. Kim, B. G. Chae, M. D. Ventra, and D. N. Basov. Phase transition driven memrisive system. *App. Phy. Lett.*, 95, 2009.

¹⁴M. J. Lee, Y. Park, D. S Suh, E. H. Lee, S. Seo, D. C. Kim, R. Jung, B. S. Kang, S. E. Ahn, C. B. Lee, D. H. Seo, Y. K. Cha, I. K. Yoo, J. S. Kim, and B. H. Park. Two series oxide resistors applicable to high speed and high density nonvolatile memory. *Adv. Mater.*, 19:3919–3923, 2007.

¹⁵G. Stefanovich, A. Pergament, and D. Stefanovich. Electrical switching and mott transition in VO₂. *J. Phys.; Condens. Matter*, 12:8837–8845, 2000.

¹⁶B. G. Chae, H. T. Kim, D. H. Youn, and K. Y. Kang. Abrupt metal insulator transition observed in VO₂ thin lms induced by a switching voltage pulse. *Physica B*, 369:76–80, 2005.

¹⁷S. Chen, H. Ma, X. Yi, H. Wang, X. Tao, M. Chen, X. Li, and C. Ke. Optical switch based on vanadium dioxide thin films. *Infra. Phys. & Tech.*, 45:239, 2004.

¹⁸R. T. K. Rajendra, B. Karunagaran, D. Mangalaraj, M. Joseph, and V. Gopal. Pulsed laser deposited vanadium oxide thin films for uncooled infrared detectors. *Sensors Actuators A*, 107:62, 2003.

¹⁹H. A. Wriedt. The O-V (oxygen-vanadium) system. *Journal of Phase Equilibria*, 10(3):271–277, 1989.

²⁰Z. Yang, C. Ko, and S. Ramanathan. Oxide electronics utilizing ultrafast metal-insulator transitions. *Annu. Rev. Mater. Res.*, 41:337–367, 2011.

²¹A. G. Rozgonyi and H. D. Hensler. Structural and electrical properties of vanadium dioxide thin films. *J. Vac. Sci. Technol.*, 5:194–199, 1968.

²²A. G. Rozgonyi and J. W. Polito. Preparation of thin films of vanadium(di-,sesqui- and pent-) oxide. *J. Electrochem. Soc.*, 115: 56–57, 1968.

²³J. Duchene, M. Terraill, and M. Pailly. Rf and dc reactive sputtering for crystalline and amorphous VO₂ thin film deposition. *Thin Solid Films*, 12:231–234, 1972.

²⁴H. Takei and S. Koide. Growth and electrical properties of vanadium-oxide single crystals by oxychloride decomposition method. *J. Phys. Soc. Japan*, 21(1010), 1996.

²⁵S. Koide and H. Takei. Epitaxial growth of VO₂ single crystals and their anisotropic properties in electrical resistivities. *J. Phys. Soc. Japan*, 22:946–947, 1967.

²⁶D. T. Manning, I. P. Parkin, R. J. H. Clark, D. Sheel, M. E. Pemble, and D. Vemadou. Intelligent window coatings: atmospheric pressure chemical vapour deposition of vanadium oxides. *J. Mater. Chem.*, 12:2936–2939, 2002.

²⁷M. Borek, F. Qian, V. Nagabushnam, and R. K. Singh. Pulsed-laser deposition of oriented VO₂ thin films on R-cut sapphire substrate. *App. Phys. Lett.*, 63:3288–3290, 1993.

²⁸H. D. Kim and S. H. Kwok. Pulsed laser deposition of VO₂ thin films. *App. Phys. Lett.*, 65:3188–3190.

²⁹M. Maaza, K. Bouziane, J. Maritz, D. S. McLachlan, R. Swanepoel, J. M. Frigerio, and M. Every. Direct production of thermochromic VO₂ thin film coatings by pulsed laser ablation. *Opt. Mater.*, 15:41–45, 2000.

³⁰B. C. Greenberg. Undoped and doped vo2 film grown from VO(OC₃H₇)₃. *Thin Solid Films*, 110:73–82, 1983.

³¹K-H Chen, H-C Huang, T C K Yang, and S-F Wang. The preparation and characterization of transparent nano-sized thermochromic VO₂-SiO₂ films from sol-gel process. *J. Non-Cryst. Solids*, 347:138–143, 2004.

³²G. B. Chae, H. T. Kim, S. J. Yun, B. J. Kim, Y. K. Lee, D. H. Youn, and K. Y. Kang. Highly oriented VO₂ thin films prepared by sol-gel deposition. *J. Kore. Phys. Soc.*, 44:884–888, 2006.

³³X. Wei, Z. Wu, and X. Xu. Growth mode and texture study in vanadium dioxide thin films deposited by magnetron sputtering. *J. Phys. D: Appl. Phys.*, 41, 2008.

³⁴D. Brassard, S. Fourmaux, and M. J. Jacques. Grain size effect on the semiconductor metal phase transition characteristics of magnetron sputtered VO₂ thin films. *App. Phys. Lett.*, 87, 2005.

³⁵RF-sputtered vanadium oxide films. *J. The Electrochem. Soc.*, 149(5), 2002.

³⁶C. H. Chen, Y. Zhao, X. Pan, V. Kuryatkov, A. Bernussi, M. Holtz, and Z. Y . Fan and. Influence of defects on structural and electrical properties of VO₂ thin films. *J. Appl. Phys.*, 110, 2011.

³⁷Z. Yang, C. Ko, and S. Ramanathan. Metal-insulator tansition characteristics of VO₂ thin films grown on ge(100) single crystals. *J. Appl. Phys.*, 108, 2010.

³⁸J. Lappalainen, S. Heinilehto, H. Jantunen, and V. Lantto. Electrical and optical properties of metal-insulator transition VO₂ thin film. *J. Electrocera.*, 22(1-3), 2009.

³⁹J. Cao and Y. Gu. Extended mapping and exploration of the vanadium dioxide stress-temperature phase diagram. *Nano Lett.*, 10:2667–2673, 2010.

⁴⁰J. Wu, Q. Gu, B. S. Guiton, N. P. de Leon, L. Ouyang, and H. Park. Strain induced self organization of metal insulator domains in single crystalline VO₂ nanobeams. *Nano Letters*, 6(10): 2313–2317, 2006.

⁴¹Y. Gu, J. Cao, J. Wu, and L. Chen. Thermodynamics of strained vanadium dioxide single crystals. *J. Appl. Phys.*, 108, 2010.

⁴²B. D. Cullity. *Elements of X-ray Diffraction*. Addison-Wesley Publishing Comapny, Inc, 1956.

⁴³K. Y. Tsai, T. S. Chin, and H. P. D. Shieh. Effect of grain curvature on nanoindentation measurements of thin films. *Jpn. J. Appl. Phys.*, 43:6268–6273, 2004.

⁴⁴M. Guntersdorfer. Conductivity anamaly in vanadium dioxide.
Solid State Electronics, 13(355-367), 1970.

⁴⁵Joost Vlassak. Thin film mechanics. Technical report, Harvard University, 2004.